Nigerian Journal of Technology (NIJOTECH)
Vol. 44, No. 4, December, 2025, pp. 590- 606
www.nijotech.com

Print ISSN: 0331-8443
Electronic ISSN: 2467-8821
https://doi.org/10.4314/njt.2025.5184

OPTIMIZATION OF AGRO-WASTE REINFORCED ALUMINIUM – BASED COMPOSITE USING D-OPTIMAL MIXTURE DESIGN

AUTHORS:
O. Oghoghorie[1*], and C. I. Eboigbe[2],

AFFILIATIONS:
[1] Department of Mechanical Engineering
Benson Idahosa University,
Benin City, Nigeria
[2] Department of Production Engineering
University of Benin, Benin City, Nigeria

***CORRESPONDING AUTHOR:**
Email: ooghoghorie@biu.edu.ng

ARTICLE HISTORY:
Received: June 17, 2025.
Revised: . September 02, 2025.
Accepted: October 10,2025.
Published: January 03, 2026.

KEYWORDS:
Agro Waste Composite, Tensile Strength, Wear Rate, Hardness, Optimization

ARTICLE INCLUDES:
Peer review

DATA AVAILABILITY:
On request from author(s)

EDITORS:
Sagar D. Shelare

FUNDING:
None

Abstract

All designers desire to use durable and reliable materials in engineering applications. In this study, a new aluminium - based composite material was produced using some agro waste materials which are Palm Kernel Shell, Bamboo Fibre, Groundnut Shell and Rice Husk as the reinforcement while aluminium scrap is the matrix. The D-Optimal mixture design was used for the experimental design. Twenty – five (25) experimental runs of the specimens were obtained from the design expert and each run was performed three times and the average was taken. A stir casting method was used in the production of the specimens. The responses tested for are Tensile strength, hardness and wear index(rate). The Numerical optimization of the input and responses was done using the design expert. The produced material was modelled using SOLIDWORKS software. SEM analysis was carried out to appropriately look at the microstructure of the composite and it was found out that the porosity seen was as a result of the casting method. It was found out that the reinforcement particles of Palm Kernel Shell, Bamboo Fibre, Groundnut Shell and Rice Husk have improved the mechanical properties of the aluminium metal. From the optimal solution obtained by the design expert, 72.43% weight of aluminium, 13.27% weight of Bamboo fibre, 12.30% weight of Rice Husk, 1.00% weight of Groundnut Shell and 1.00% weight of Palm kernel shell can be used to produce an Engineering composite material with a tensile strength of 241.23 MPa, hardness of 114.07 HV and wear index(rate) of 0.18 x 10^{-3} mg/rpm with a desirability of 88.3% which is applicable in the production of automobile components.

1.0 INTRODUCTION

Design engineers and other experts are now paying increasing attention to the use of materials that offer an optimal combination of low wear rate, good corrosion resistance, lightweight, cost-effectiveness, and durability when designing components for automobiles and other machines [1]. Research has shown that no single engineering material can simultaneously meet all of these desired mechanical properties, such as low wear rate, high tensile strength and high hardness, while also exhibiting a reduction in density according to [2]. Consequently, the use of composite materials is essential in overcoming these limitations. Various researchers have developed locally sourced materials for producing components that meet the specific needs of engineering applications. [3] Conducted a detailed design and analysis of an 80cc, 4-stroke spark ignition engine connecting rod, emphasizing the

HOW TO CITE:
Oghoghorie, O. and Eboigbe, C. I. "Optimization of Agro-Waste Reinforced Aluminium – Based Composite Using D-Optimal Mixture Design", *Nigerian Journal of Technology*, 2025. 44(4), pp. 590- 590. https://doi.org/10.4314/njt.2025.5184

importance of material selection in achieving a balance between strength, weight, and durability in engine components. In a similar vein, Metal matrix composites MMCs are used to manufacture car parts, airplane frames, and jet engines—components that require both strength and reduced weight [4]. To achieve high strength, metallic matrix materials often require high-modulus reinforcements, and the resulting composites can surpass most alloys in terms of strength-to-weight ratios [5].

2.0 MATERIALS AND METHODS

2.1 Materials

In this research, agricultural waste that comprises Palm Kernel Shell, Bamboo Fibre, Rice Husk and Groundnut Shell were used as reinforcements on Aluminium Scrap which is the Matrix element to develop a composite material locally. Magnesium metal powder was used as the wetting agent to encourage proper bonding of the material

2.2 Methods

2.2.1 Design of experiment (DOE) using d-optimal mixture design

An experimental plan for this study was designed using a five-variable mixture design. This approach is the most appropriate for optimizing formulation processes where the input factors are the components of the product being developed according to [6]. D-Optimal design was specifically chosen due to the constraints involved and because it requires fewer experimental runs than a simplex design. The default lower bounded pseudo values (L_Pseudo) were used to fill the design space. Table 1 displays the range of the actual input factors. In a mixture design, the levels of the input factors are interdependent since they are parts of a mixture or formulation. Therefore, for the three-component mixture examined in this research, the constraint is defined as shown in Equation 1 and the summability of the components is in Equation 2.

$$0 \leq A, \ldots., E \leq 100 \quad (1)$$

$$A + B + C + D + E = 100 \quad (2)$$

Table 2 shows the Experimental Design Matrix which clearly show the ratios at which the reinforcements were added to the Matrix elements.

Table 1: Coded and actual levels of the factors

Factors	Symbols	Units	Variable levels	
			Low level	High level
Aluminum scrap	A	%	69	96
Bamboo fiber	B	%	1	20
Rice husk	C	%	1	20
Groundnut shell	D	%	1	20
Palm kernel shell	E	%	1	20

Table 2: Experimental design matrix

Run	Factors				
	Aluminum scrap (%)	Bamboo fiber (%)	Rice husk (%)	Groundnut shell (%)	Palm kernel shell (%)
1	84.1	1.0	1.0	1.0	12.9
2	83.6	1.0	1.0	13.4	1.0
3	74.8	4.0	4.8	13.4	3.0
4	69.0	15.7	1.0	13.2	1.0
5	87.3	4.4	2.7	4.6	1.0
6	77.5	1.0	9.6	1.0	10.8
7	96.0	1.0	1.0	1.0	1.0
8	69.0	1.0	9.7	19.3	1.0

https://doi.org/10.4314/njt.2025.5184
http://creativecommons.org/licenses/by-nc-nd/4.0/

9	69.0	19.0	1.0	1.0	9.9
10	69.0	15.7	1.0	13.2	1.0
11	69.5	2.7	1.7	6.1	20.0
12	69.0	19.9	9.0	1.0	1.0
13	76.7	7.6	2.9	5.3	7.5
14	69.0	10.0	10.5	1.0	9.4
15	84.0	1.0	13.0	1.0	1.0
16	69.0	1.0	1.0	19.3	9.7
17	69.0	6.3	19.8	3.9	1.0
18	69.0	6.3	19.8	3.9	1.0
19	69.0	1.0	16.3	1.0	12.6
20	69.0	1.0	7.8	11.2	11.0
21	83.9	13.1	1.0	1.0	1.0
22	69.0	19.0	1.0	1.0	9.9
23	69.0	8.1	3.7	6.6	12.6
24	69.5	2.7	1.7	6.1	20.0
25	69.0	1.0	1.0	19.3	9.7

2.2.2 Stir casting rig and the crucible

The Stir Casting Rig was used in this research. The different Reinforcements were added to the matrix in the ratios given by the design expert as shown Table 2, after stirring the matrix material for about 20mins. The wetting agent used in this research is pure magnesium to encourage proper bonding of the material. Each run was performed three times and the average was taken. A stir casting method was used in the production of the specimens.

2.2.3 Green sand mould

In this study, Green Sand that was used consists of silica sand and mixed together uniformly with about 20% clay and 7% water. Figure 1 shows the Green Sand Mould.

Figure 1: Green sand mould

2.2.4 Statistical modelling

To develop statistical models for the three responses, the linear, quadratic, special cubic, and cubic models from the Design Expert model library were evaluated for their appropriateness. Equation 3 represents the linear model, which includes the design space vertices, edge centers, the overall centroid and the axial points positioned midway between the overall centroid and the vertices.

$$Y = \sum_{i=1}^{N} b_i X_i \quad (3)$$

Where Y_i is the dependent variable or predicted response, X_i is the independent variables, b_o is offset term, b_i is the regression coefficient and e_i is the error term.

The quadratic model shown in Equation 4, incorporates the vertices of the design space, the edge centers, the constraint plane centroids, the overall centroid, and the axial points.

$$Y = \sum_{i=1}^{N} b_i X_i + \sum_{i,j=1}^{N} b_{ij} X_i X_j \quad (4)$$

X_j is the independent variables or factors while b_{ij} is the coefficient of the interaction terms.
For the special cubic and cubic model, the candidate points incorporate the vertices, the thirds of edges, the constraint plane centroids, the overall centroid, and the axial points as shown in Equations 5 and 6.

https://doi.org/10.4314/njt.2025.5184

$$Y = \sum_{i=1}^{N} b_i X_i + \sum_{i,j=1}^{N} b_{ij} X_i X_j + \sum_{i=1}^{N} b_{ijk} X_i X_j X_k \quad (5)$$

$$Y = \sum_{i=1}^{N} b_i X_i + \sum_{i,j=1}^{N} b_{ij} X_i X_j + \sum_{i=1}^{N} b_{ijk} X_i X_j X_k + \sum_{i=1}^{N} b_{ij} X_i X_j (X_i - X_j) \quad (6)$$

2.2.5 Analysis of formulated models

The models developed to predict the three responses underwent statistical analysis to evaluate how well they aligned with the actual experimental data. This evaluation was conducted using the analysis of variance (ANOVA) feature in the Design Expert software. The ANOVA parameters employed included p value, F value, sum of squares, mean square, lack of fit, standard deviation, coefficient of variation, coefficient of determination (R^2), adjusted R^2, adequate precision, and predicted residual sum of squares (PRESS). The F value is a statistical measure that contrasts the variance linked to a model term with the residual variance. The p value represents the probability associated with the F value for a specific model term, indicating the likelihood of obtaining an F value if the term had no impact on the response. Typically, terms with a p value below 0.05 are considered significant; otherwise, they are not. The coefficient of determination (R^2) quantifies the proportion of variation around the mean that the model accounts for. Conversely, the adjusted R^2 value is the R^2 value modified to account for the number of terms in the model, decreasing with the addition of non-significant terms. Ideally, both the R^2 and adjusted R^2 values should be as close to one as possible [7]. A value of 1.0 signifies the perfect scenario where the model explains 100 percent of the variation in the observed values.

2.2.6 Numerical optimization

The responses and their corresponding input factors were numerically optimized using a desirability criterion using the Design Expert software. The responses indicating favorable performance for the formulation, such as tensile strength and hardness were maximized, while those indicating less favorable performance, like wear index was minimized.

2.2.7 Wear rate test

In this study, ASTM D4060 standard specification was used in Taber Abrasive machine. A load of 5.0KN was applied in 10secs at 500rpm. The loss in weight was determined for each sample and the Wear Index was calculated for using equation 7

$$\text{Wear Index}(W.I) = \frac{(M)\times 1000}{RPM} \quad (7)$$

2.2.8 Hardness test results

The ASTM E384 standard Vickers hardness test was used in this study. A load of 100gf was applied for 10secs. The Vickers number for each sample as was calculated for using equation 8

$$VHN = \frac{P}{As} = \frac{2000P\sin\left(\frac{a}{2}\right)}{d^2} \quad (8)$$

Figure 2: Specimen for wear rate test

2.2.9 Tensile strength test

The standard that was used in this test is in accordance with the ASTM B557. The tensile strength values were determined by using equations 9 and 10 respectively. Mathematically,

$$\text{Tension} = \frac{\text{Maximum Load}}{\text{Original Cross-Sectional Area}} \quad (9)$$

$$\text{Cross} - \text{Section Area} = \frac{\pi d^2}{4} \quad (10)$$

Where d = Diameter

3.0 RESULTS AND DISCUSSION

3.1 Statistical Modelling

3.1.1 Assessment of the experimental design

Table 3 shows the summary of the Factors and Responses of the Developed Composite Material while the standard errors associated with the design

https://doi.org/10.4314/njt.2025.5184
http://creativecommons.org/licenses/by-nc-nd/4.0/

model are presented in Table 4 and the results indicate that the standard errors of the model terms are relatively small, suggesting that the estimates are robust and that the model provides reliable predictions.

Table 3 shows the summary of the Factors and Responses of the Developed Composite Material while the standard errors associated with the design model are presented in Table 4 and the results indicate that the standard errors of the model terms are relatively small, suggesting that the estimates are robust and that the model provides reliable predictions. The VIF values reported in Table 4 shows that the majority of the model terms exhibit relatively low VIF values, thereby confirming the orthogonality of the design and ensuring that multicollinearity does not significantly affect the model's predictive accuracy according to [8]. The maximum leverage value recorded in Table 5 is below unity, indicating that no experimental runs exhibit extreme leverage that could compromise the validity of the results according to [9].

Table 3: The summary of the factors and responses of the developed composite

	Factors					Responses		
	Aluminum scrap (%)	**Bamboo fiber (%)**	**Rice husk (%)**	**Groundnut shell (%)**	**Palm kernel shell (%)**	**Tensile strength (MPa)**	**Hardness (HV)**	**Wear Index (10^{-3}) (mg/rpm)**
1	84.1	1.0	1.0	1.0	12.9	267.34	85.7	1.738
2	83.6	1.0	1.0	13.4	1.0	254.61	91.6	1.848
3	74.8	4.0	4.8	13.4	3.0	257.80	96.1	1.200
4	69.0	15.7	1.0	13.2	1.0	216.42	111.2	1.536
5	87.3	4.4	2.7	4.6	1.0	292.21	93.8	0.718
6	77.5	1.0	9.6	1.0	10.8	269.93	95.3	0.712
7	96.0	1.0	1.0	1.0	1.0	143.95	86.0	1.664
8	69.0	1.0	9.7	19.3	1.0	190.21	85.3	1.716
9	69.0	19.0	1.0	1.0	9.9	143.95	83.9	1.744
10	69.0	15.7	1.0	13.2	1.0	216.42	77.2	0.530
11	69.5	2.7	1.7	6.1	20.0	143.38	96.4	1.580
12	69.0	19.9	9.0	1.0	1.0	262.61	101.2	0.334
13	76.7	7.6	2.9	5.3	7.5	249.43	93.5	1.406
14	69.0	10.0	10.5	1.0	9.4	203.28	120.7	1.246
15	84.0	1.0	13.0	1.0	1.0	237.68	85.2	0.302
16	69.0	1.0	1.0	19.3	9.7	270.99	92.7	0.516
17	69.0	6.3	19.8	3.9	1.0	224.95	109.7	0.422
18	69.0	6.3	19.8	3.9	1.0	219.31	108.9	1.470
19	69.0	1.0	16.3	1.0	12.6	237.20	97.8	1.792
20	69.0	1.0	7.8	11.2	11.0	249.43	87.9	1.704
21	83.9	13.1	1.0	1.0	1.0	246.06	103.1	1.780
22	69.0	19.0	1.0	1.0	9.9	262.61	104.8	1.340
23	69.0	8.1	3.7	6.6	12.6	216.42	85.9	1.328
24	69.5	2.7	1.7	6.1	20.0	245.12	78.9	1.616
25	69.0	1.0	1.0	19.3	9.7	232.88	89.3	1.188

https://doi.org/10.4314/njt.2025.5184
http://creativecommons.org/licenses/by-nc-nd/4.0/

Table 4: Estimated standard error of design model terms

Term	Standard error	VIF	R_i^2	Power at 5 % alpha level for effect of		
				0.5 Std. Dev.	1 Std. Dev.	2 Std. Dev.
A	0.96	2.66	0.62	5.8%	8.3%	18.4%
B	2.59	17.05	0.94	5.2%	6.0%	8.9%
C	2.34	11.05	0.91	5.4%	6.5%	11.2%
D	3.02	23.04	0.96	5.2%	5.9%	8.8%
E	2.50	15.12	0.93	5.4%	6.6%	11.5%
AB	6.17	2.81	0.64	6.0%	9.1%	21.7%
AC	5.74	2.44	0.59	6.2%	9.7%	24.3%
AD	6.68	3.64	0.73	5.9%	8.4%	19.2%
AE	5.93	2.79	0.64	6.1%	9.4%	23.1%
BC	9.94	9.51	0.89	5.4%	6.5%	11.3%
BD	6.23	5.09	0.80	6.0%	9.0%	21.4%
BE	7.85	7.94	0.87	5.6%	7.5%	15.2%
CD	9.42	6.46	0.85	5.4%	6.7%	12.0%
CE	6.54	4.17	0.76	5.9%	8.6%	19.8%

Table 5: Estimated model leverages

Standard order	Leverage
1	0.91
2	0.83
3	0.95
4	0.83
5	0.49
6	0.49
7	0.49
8	0.83
9	0.89
10	0.49
11	0.49
12	0.80
13	0.73
14	0.94
15	0.88
16	0.30
17	0.24
18	0.37
19	0.25
20	0.35
21	0.49
22	0.49
23	0.49
24	0.49
25	0.49

Tables 6 and 7 present the correlation matrix of regression coefficients and the Pearson's correlation matrix of experimental factors, respectively. The results in Table 6 show that most off-diagonal values are relatively small, suggesting that the regression coefficients are largely independent, thereby enhancing the reliability of the model. Table 7 indicate that the majority of correlations between factors remain low, suggesting that the experimental design effectively mitigates strong interdependencies among the predictor variables. Table 8 presents the degrees of freedom associated with various components of the experimental design model. The model accounts for 14 degrees of freedom, while the residuals contribute 10 degrees of freedom. Both the lack-of-fit and pure error terms have 5 degrees of freedom each, culminating in a total of 24 degrees of freedom when considering the corrected totals. The adequacy of an experimental design is frequently evaluated by examining the degrees of freedom allocated to lack of fit and pure error. it is recommended that the degrees of freedom for lack of fit and pure error should be at least 3 and 4, respectiv

https://doi.org/10.4314/njt.2025.5184
http://creativecommons.org/licenses/by-nc-nd/4.0/

Table 6: Correlation matrix of regression coefficient

	A	B	C	D	E	AB	AC	AD	AE	BC	BD	BE	CD	CE	DE
A	1														
B	-0.03	1.00													
C	-0.04	0.31	1.00												
D	-0.02	-0.43	-0.04	1.00											
E	-0.03	-0.14	-0.04	0.55	1.00										
AB	-0.34	-0.70	-0.17	0.39	0.18	1.00									
AC	-0.33	-0.20	-0.66	0.05	0.07	0.22	1.00								
AD	-0.30	0.43	0.12	-0.77	-0.40	-0.30	-0.01	1							
AE	-0.28	0.14	0.10	-0.39	-0.72	-0.06	-0.05	0.37	1.00						
BC	0.03	-0.77	-0.74	0.36	0.16	0.52	0.50	-0.38	-0.18	1.00					
BD	0.05	-0.49	-0.24	-0.46	-0.34	0.26	0.12	0.26	0.19	0.35	1.00				
BE	0.04	-0.79	-0.18	0.15	-0.37	0.51	0.10	-0.21	0.23	0.53	0.54	1.00			
CD	0.04	0.28	-0.42	-0.79	-0.39	-0.29	0.25	0.56	0.24	-0.03	0.41	-0.11	1.00		
CE	0.07	-0.06	-0.61	-0.27	-0.57	-0.04	0.33	0.14	0.32	0.33	0.28	0.27	0.46	1.00	
DE	0.03	0.39	0.09	-0.89	-0.81	-0.37	-0.09	0.68	0.58	-0.35	0.40	0.02	0.65	0.39	1.00

https://doi.org/10.4314/njt.2025.5184

Table 7: Correlation matrix of factor

	A	B	C	D	E	AB	AC	AD	AE	BC	BD	BE	CD	CE	DE
A	1														
B	-0.32	1.00													
C	-0.25	-0.17	1.00												
D	-0.31	-0.27	-0.27	1.00											
E	-0.34	-0.22	-0.22	-0.11	1.00										
AB	0.38	0.17	-0.21	-0.19	-0.25	1.00									
AC	0.35	-0.25	0.25	-0.23	-0.17	-0.03	1.00								
AD	0.36	-0.21	-0.21	0.24	-0.27	0.07	-0.01	1							
AE	0.29	-0.24	-0.13	-0.25	0.28	-0.04	0.08	-0.06	1.00						
BC	-0.29	0.34	0.59	-0.29	-0.28	-0.13	-0.15	-0.13	-0.15	1.00					
BD	-0.22	0.40	-0.22	0.31	-0.27	-0.08	-0.11	-0.06	-0.11	-0.11	1.00				
BE	-0.30	0.55	-0.24	-0.32	0.36	-0.12	-0.16	-0.14	-0.12	-0.06	-0.13	1.00			
CD	-0.25	-0.25	0.41	0.40	-0.24	-0.11	-0.12	-0.06	-0.14	0.10	-0.10	-0.19	1.00		
CE	-0.21	-0.24	0.41	-0.25	0.38	-0.14	0.01	-0.15	0.03	-0.04	-0.17	-0.03	-0.07	1.00	
DE	-0.34	-0.37	-0.30	0.55	0.55	-0.15	-0.18	-0.15	-0.14	-0.24	-0.15	-0.07	-0.05	-0.04	

https://doi.org/10.4314/njt.2025.5184
http://creativecommons.org/licenses/by-nc-nd/4.0/

In this study, both lack of fit and pure error possesses 5 degrees of freedom, exceeding the minimum recommendations and indicating a robust experimental design.

Table 8: Degrees of Freedom for Statistics

Term	Value
Model	14
Residuals	10
Lack of fit	5
Pure error	5
Corrected totals	24

3.1.2. Selection of suitable statistical models

In this study, the model fit and lack-of-fit test results were evaluated for tensile strength, hardness, and wear index. Tables 9 and 10 present the model summary and lack-of-fit test results for the tensile strength of the composite material. The quadratic model emerged as the most suitable choice for modeling tensile strength, as it exhibited the highest R^2 value (0.9016), the lowest standard deviation (14.5078), and the lowest PRESS value (8895.665) compared to other models (Table 9). The special cubic and cubic models were aliased, indicating an insufficient number of experimental runs to estimate their parameters effectively. Furthermore, the lack-of-fit test results (Table 10) confirmed that the quadratic model exhibited no significant lack of fit ($p = 0.9990$), which is desirable in regression modeling [6]. A non-significant p-value ($p > 0.05$) suggests that the model adequately represents the experimental data. Based on these statistical criteria, the quadratic model was selected as the best fit for predicting the tensile strength of the composite material. The statistical evaluation for modeling the hardness of the composite material is presented in Tables 11 and 12. The quadratic model was again determined to be the most suitable, as it demonstrated a high R^2 value (0.9094), adjusted R^2 value (0.7825), and predicted R^2 value (0.5812), along with the lowest standard deviation (4.0837) and PRESS (770.628) among all the models assessed (Table 11). Although the special cubic model had the highest R^2 value (0.9121), it was identified as aliased, indicating that the available experimental data were insufficient to estimate its parameters reliably [10]. The lack-of-fit test results (Table 12) further supported the quadratic model, as it exhibited a non-significant lack of fit ($p = 0.9991$), confirming its adequacy for predicting the hardness of the composite material. The suitability of the statistical models for predicting the wear index of the composite material is summarized in Tables 13 and 14. Similar to the findings for tensile strength and hardness, the quadratic model was found to be the most appropriate, as it exhibited a high R^2 value (0.9648), adjusted R^2 value (0.9156), and predicted R^2 value (0.7635), along with the lowest standard deviation (0.1282) and PRESS value (1.1043) (Table 13). Although the special cubic model had a slightly higher R^2 value (0.9705), it was also identified as aliased, indicating that the model parameters could not be accurately estimated due to an insufficient number of experiments. The lack-of-fit test (Table14) confirmed the quadratic model as the best choice, as it exhibited a non-significant lack of fit ($p = 0.9530$), while all other models displayed p-values less than 0.05, indicating poor fit [11].

Table 9: Summary of model fit results for tensile strength

Source	Standard deviation	R^2	Adjusted R^2	Predicted R^2	PRESS	Remark
Linear	32.57853	0.007422	-0.19109	-0.80752	38655.52	
Quadratic	14.50779	0.901582	0.763797	0.584041	8895.665	Suggested
Special cubic	20.18672	0.904726	0.542686		+	Aliased
Cubic					+	Aliased

https://doi.org/10.4314/njt.2025.5184
http://creativecommons.org/licenses/by-nc-nd/4.0/

Table 10: Lack of fit test results for tensile strength

Source	Sum of squares	degree of freedom	Mean square	F-value	p value	Remark
Linear	19189.69	15	1279.313	3.139389	0.1059	
Quadratic	67.24192	5	13.44838	0.033002	0.9990	Suggested
Special cubic	0	0				Aliased
Cubic	0	0				Aliased
Pure Error	2037.519	5	407.5037			

Table 11: Summary of model fit results for hardness

Source	Standard deviation	R^2	Adjusted R^2	Predicted R^2	PRESS	Remark
Linear	6.465426	0.545626	0.454751	0.308894	1271.614	
Quadratic	4.083656	0.909367	0.78248	0.581173	770.6279	Suggested
Special cubic	5.685908	0.912146	0.578303		+	Aliased
Cubic					+	Aliased

Table 12: Lack of fit test results for hardness

Source	Sum of squares	degree of freedom	Mean square	F-value	p value	Remark
Linear	674.3869	15	44.95913	1.390651	0.3809	
Quadratic	5.11474	5	1.022948	0.031641	0.9991	Suggested
Special cubic	0	0				Aliased
Cubic	0	0				Aliased
Pure Error	161.6478	5	32.32955			

Table 13: Summary of model fit results for wear index

Source	Standard deviation	R^2	Adjusted R^2	Predicted R^2	PRESS	Remark
Linear	0.429315	0.210535	0.052642	-0.30767	6.1059	
Quadratic	0.128175	0.964815	0.915556	0.763487	1.104346	Suggested
Special cubic	0.166049	0.970475	0.85828		+	Aliased
Cubic					+	Aliased

Table 14: Lack of fit test results for wear index

Source	Sum of squares	degree of freedom	Mean square	F-value	p value	Remark
Linear	3.548375	15	0.236558	8.579623	0.0133	
Quadratic	0.026428	5	0.005286	0.191698	0.9530	Suggested
Special cubic	0	0				Aliased
Cubic	0	0				Aliased
Pure Error	0.137861	5	0.027572			

3.1.3. Analysis of variance of the statistical models

https://doi.org/10.4314/njt.2025.5184
http://creativecommons.org/licenses/by-nc-nd/4.0/

A quadratic model was selected and fitted to the experimental data obtained from 25 experimental runs, following a D-Optimal mixture design. The primary objective of fitting the quadratic model was to estimate the unknown model parameters, which was accomplished through multiple regression analysis [12, 16]. By substituting the estimated parameters into the general form of the response surface methodology (RSM) models, the final predictive equations for tensile strength, hardness, and wear index were derived. These models describe the responses as functions of the percentage composition of aluminum scrap (A), bamboo fiber (B), rice husk (C), groundnut shell (D), and palm kernel shell (E), as presented in Equations 11 to 13.

$$\text{Tensile strength} = 0.95A + 8.45B - 13.69C - 49.31D - 55.42E + 0.030AB + 0.28AC + 0.72AD + 0.79AE - 0.36BC - 0.16BD - 0.17BE + 0.18CD + 0.34CE + 0.84DE \quad (11)$$

$$\text{Hardness} = 0.83A - 9.91B + 4.06C + 5.76D + 1.40E + 0.14AB - 0.037AC - 0.049AD - 0.0063AE + 0.18BC + 0.064BD + 0.12BE - 0.16CD + 0.030CE - 0.12DE \quad (12)$$

$$\text{Wear index} = 0.018A + 0.017B + 0.65C - 0.17D + 0.13E - 0.000011AB - 0.0091AC - 0.0023AD - 0.0012AE - 0.0078BC - 0.00032BD - 0.0011BE + 0.0026CD\ 0.0010CE - 0.0036DE \quad (13)$$

3.1.4. Analysis of variance of models

Table 15 shows the Goodness of fit statistics for all three responses. The obtained R2 values were close to unity. This indicates that there was a very good fit between the model and the experimental results while the SD values were far less than the mean values and the CV values were below 10. This shows the accuracy of the model and the high reliability of the experiment respectively.

Table 15: Goodness of fit statistics for all three responses

Parameter	Value for each response		
	Tensile strength	Hardness	Wear index
R^2	0.9016	0.9094	0.9648
Adjusted R^2	0.7638	0.7825	0.9156
Predicted R^2	0.5840	0.5812	0.7635
Mean	231.500	95.270	1.2900
Standard deviation	14.5100	4.0800	0.1300
C.V %	6.2700	4.2900	9.9300
Adequate precision	10.198	9.6830	17.984

3.2 Scanning Electron Microscope (SEM)

From the SEM analysis, it can be seen that there is a porosity that was caused by the casting method used. This will negatively affect the mechanical properties of the composite. The chemical elements present in the composite are shown in EDX in Figure 4

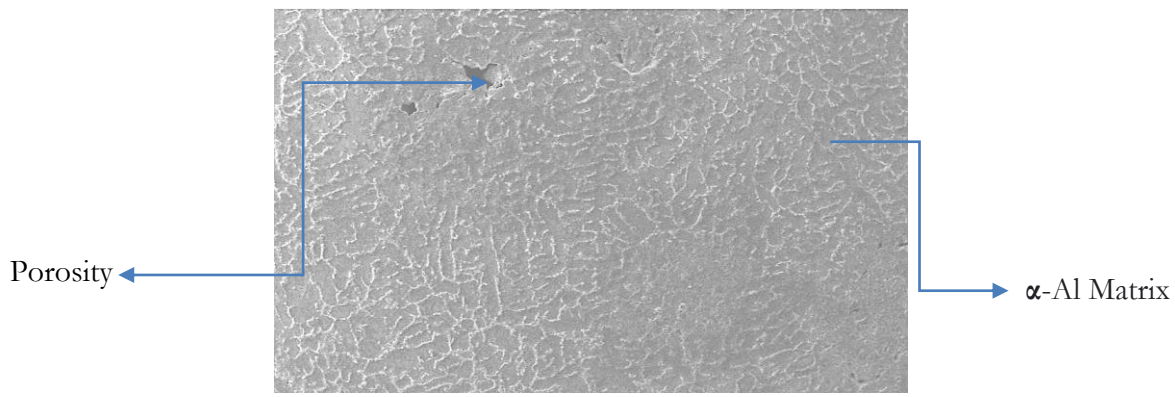

https://doi.org/10.4314/njt.2025.5184
http://creativecommons.org/licenses/by-nc-nd/4.0/

Figure 3: SEM result of the optimum sample (72.43% of Aluminium matrix, 13.27% of Bamboo fibre, 12.30% of Rice Husk, 1.00% of Groundnut Shell, and 1.00% of Palm Kernel Shell)

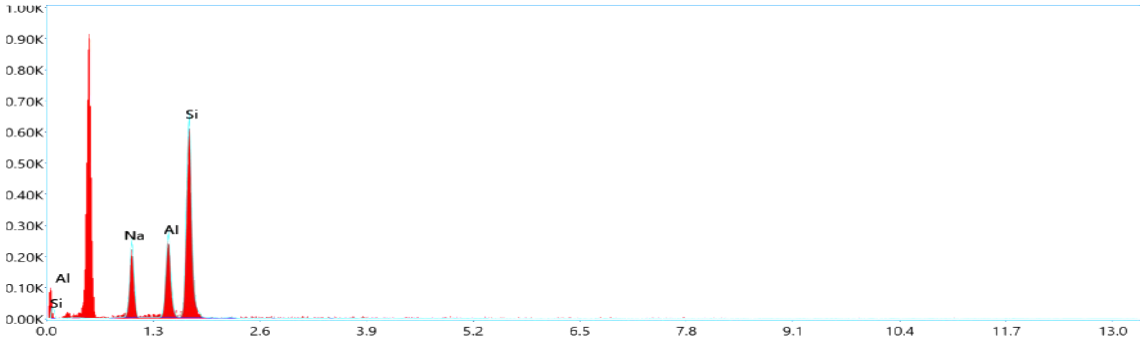

Smart Quant Results

Element	Weight %	Atomic %	Net Int.	Error %	R	A	F
NaK	19.30	22.43	27.99	8.61	0.9075	0.5423	1.0101
AlK	20.49	20.29	35.42	7.93	0.9160	0.5867	1.0208
SiK	60.21	57.28	89.44	7.14	0.9199	0.5327	1.0018

Figure 4: EDX result of the optimum sample (72.43% of Aluminium matrix, 13.27% of Bamboo fibre, 12.30% of Rice Husk, 1.00% of Groundnut Shell, and 1.00% of Palm Kernel Shell)

3. 3 Response Surface Plots

3D response surface plots were employed to analyze the influence aluminum scrap, bamboo fiber, rice husk, groundnut shell, and palm kernel shells on the mechanical properties of the developed composite. Figure 5 presents the 3D response surface plot illustrating the impact of aluminum scrap, bamboo fiber, and rice husk composition on the tensile strength of the composite material. The observed trend indicates that intermediate levels of aluminum scrap positively influenced tensile strength, whereas excessively low or high amounts led to a decline in tensile strength. This suggests that an optimal range of aluminum scrap is necessary to enhance mechanical performance. Additionally, increasing the bamboo fiber and rice husk content contributed to an improvement in tensile strength, highlighting their reinforcing effect. This can be attributed to the inherent mechanical properties of these lignocellulosic materials, which enhance load-bearing capacity and structural integrity in metal-matrix composites [13]. This aligns with findings from literature, where aluminum-based composites reinforced with agricultural waste materials demonstrated enhanced mechanical properties due to the presence of hard ceramic phases in the reinforcements [14].

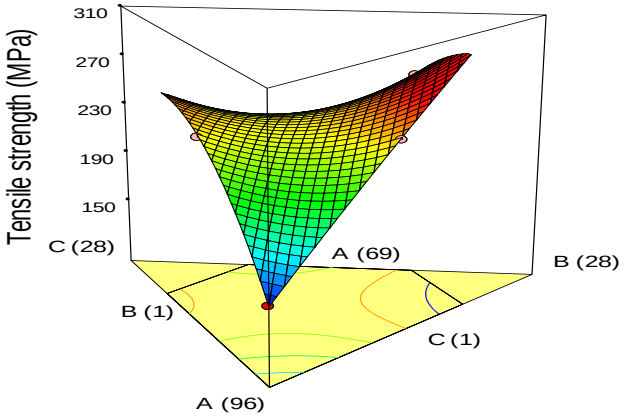

Figure 5: 3D plot showing the effect A= aluminum scrap; B= bamboo fiber; C = rice husk on tensile strength

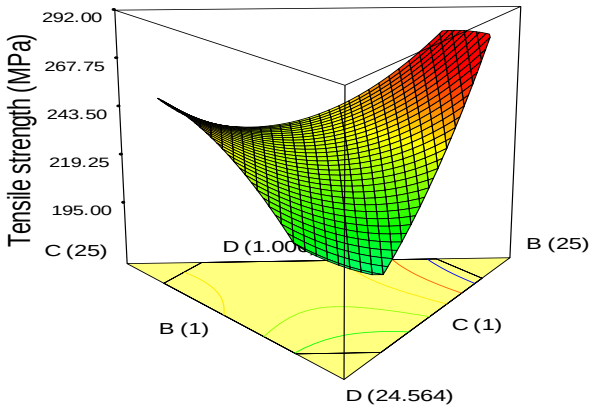

Figure 6: 3D plot showing the effect A= aluminum scrap; B= bamboo fiber; D = groundnut shell on tensile strength

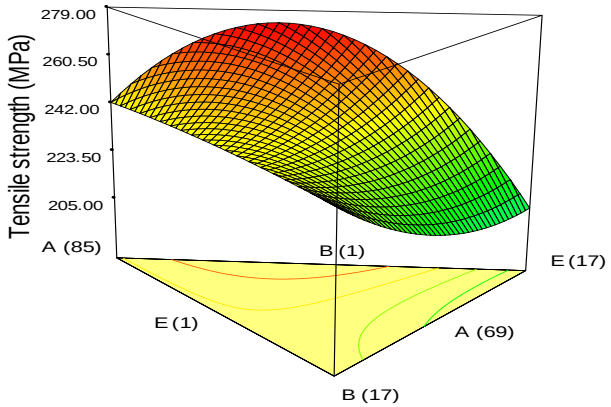

Figure 7: 3D plot showing the effect A= aluminum scrap; B= bamboo fiber; E = palm kernel shell on tensile strength

In the 3D response surface plot, different color regions indicate variations in tensile strength across the design space. The red regions correspond to areas of high tensile strength, while the blue regions represent lower tensile strength values. The green region signifies intermediate tensile strength values, suggesting that the mechanical properties of the composite can be optimized by appropriately adjusting the composition of aluminum scrap, bamboo fiber, and rice husk. These findings provide crucial insights into the formulation of aluminum-based composites and the potential of agro-waste reinforcements for enhancing mechanical performance. The trends in Figures 6 and 7 show that groundnut shell and palm kernel shells also played some reinforcing roles in the composite in alignment with previous studies ([15], [16], [17], [18]). Figure 8 presents the 3D plot illustrating the effect of A, B and C on the hardness of the developed composite material. The observed trend suggests that lower concentrations of aluminum scrap contribute to increased hardness, while intermediate levels of bamboo fiber and rice husk enhance the composite's hardness. This implies that excessive amounts of aluminum scrap may weaken the composite matrix, likely due to reduced reinforcement from the organic fillers, whereas an optimal balance of bamboo fiber and rice husk strengthens the material structure. Figures 9 and 10 show the influence of groundnut shell and palm kernel shell content on hardness. The results indicate that lower proportions of these components favor higher hardness values. This trend aligns with findings from previous studies, where excessive inclusion of lignocellulosic reinforcements has been shown to lead to reduced compaction and weaker interfacial bonding, thereby diminishing hardness [19, 20]. Conversely, moderate levels of fiber and husk reinforcement enhance load distribution and mechanical stability, which contributes to improved hardness characteristics.

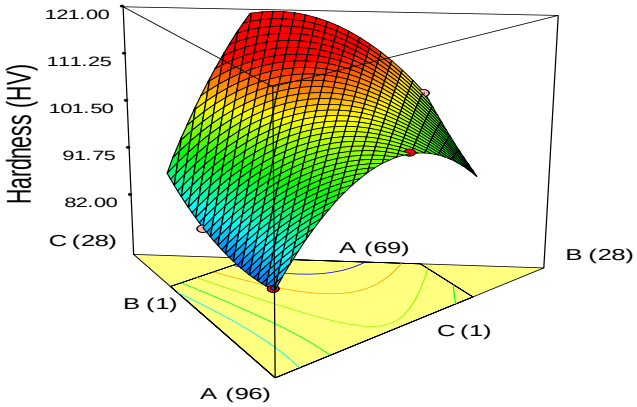

Figure 8: Plot showing the effect of A= aluminum scrap; B= bamboo fiber; C = rice husk on hardness

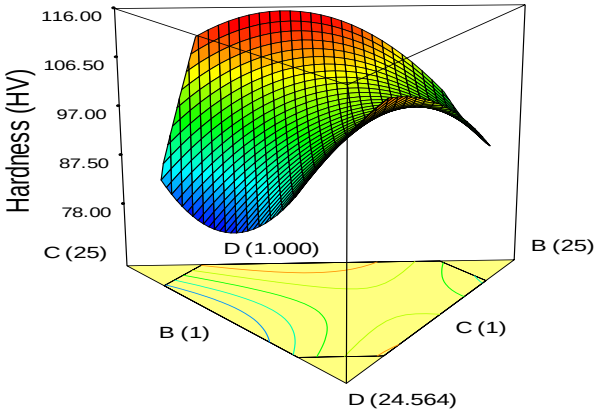

Figure 9: Plot showing effect of A= aluminum scrap; B= bamboo fiber; D = groundnut shell on hardness

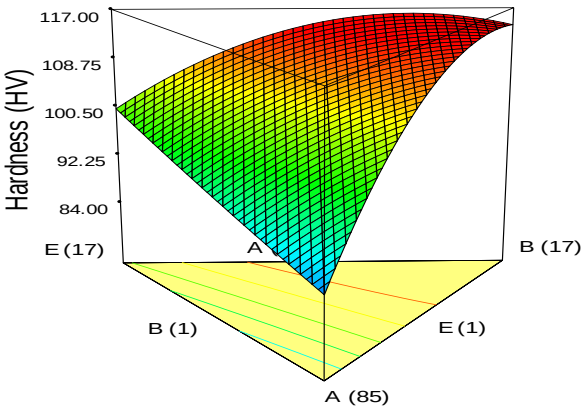

Figure 10: Plot showing the effect of A= aluminum B= bamboo fiber; E = palm kernel shell on hardness

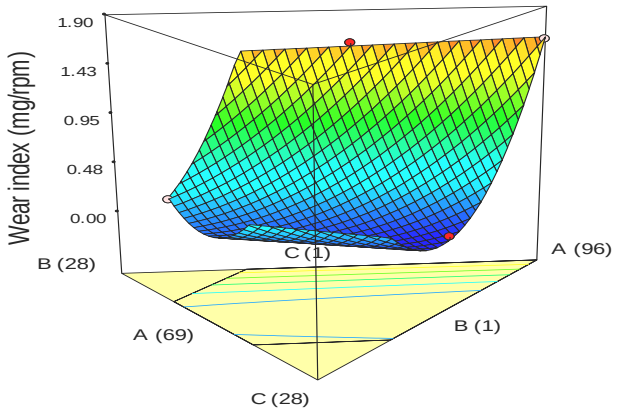

Figure 11: 3D plot showing the effect of A= aluminum scrap;B= bamboo fiber; C = rice husk on wear index

The three-dimensional response surface plots presented in Figures 11 to 12 illustrate the impact of varying proportions of aluminum scrap, bamboo fiber, rice husk, groundnut shell, and palm kernel shell on the wear index of the composite material. As a lower wear index is indicative of enhanced wear resistance, these plots provide valuable insights into the optimal composition required to minimize wear. The results indicate that the minimum wear index values, represented by the blue regions of the response surface plots, were achieved when the composite contained high amounts of rice husk while maintaining relatively low levels of aluminum scrap (Figure 11), low levels of groundnut shell (Figure 12), and low levels of palm kernel shell (Figure 13). This mean that rice husk plays an important role in enhancing the wear resistance of the composite, potentially due to its high silica content, which contributes to hardness and reduces material degradation under frictional forces [21]. Similar findings have been reported in previous studies, where rice husk reinforcements improved the wear properties of aluminum matrix composites [22, 23]. Additionally, the minimal presence of groundnut shell and palm kernel shell in the optimal composition suggests that these organic reinforcements may not significantly contribute to improving wear resistance compared to the effect observed with rice husk. The observed trends emphasize the importance of selecting appropriate reinforcement proportions to optimize wear properties in aluminum matrix composites.

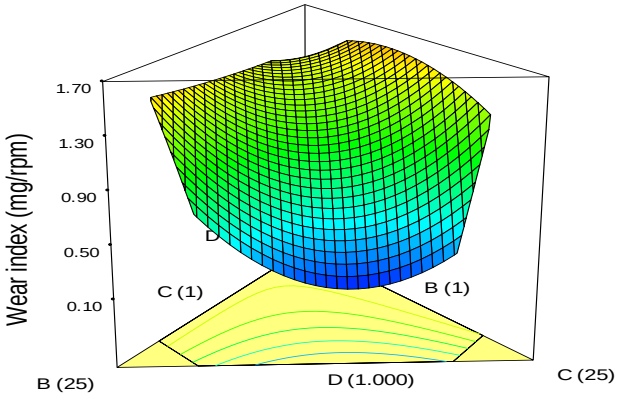

Figure 12: 3D plot showing the effect of A= aluminum scrap; B= bamboo fiber; D = groundnut shell on wear index

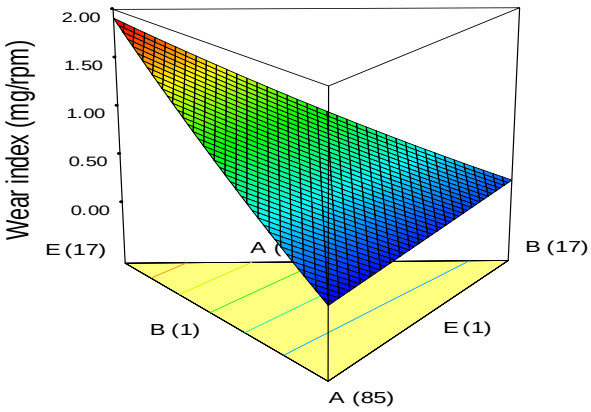

Figure13: 3D plot showing the effect of A= aluminum scrap; B= bamboo fiber; E = palm kernel shell on wear index

3.4 Numerical Optimization of Input Factors and Responses

Numerical optimization was carried out utilizing the built-in optimization algorithm of Design-Expert software to identify the optimal levels of input factors that optimized the desired mechanical properties of the composite material. Figures 14 to 16 show the optimization steps for the input factors while figure 17 shows the solution to the optimization problem. Table 19 shows the constraints for numerical optimization.

https://doi.org/10.4314/njt.2025.5184
http://creativecommons.org/licenses/by-nc-nd/4.0/

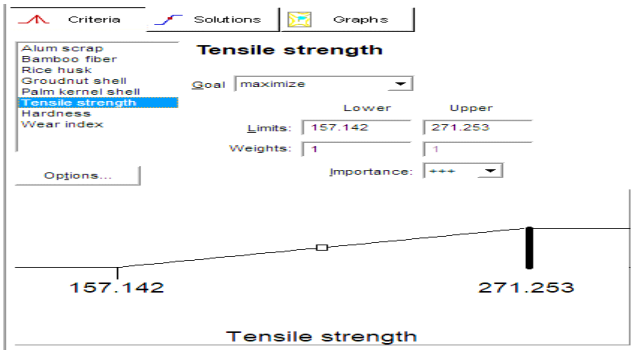

Figure 14: Optimization step for tensile strength

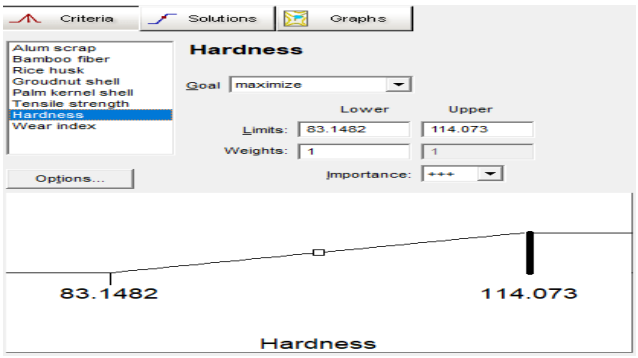

Figure 15: Optimization step for hardness

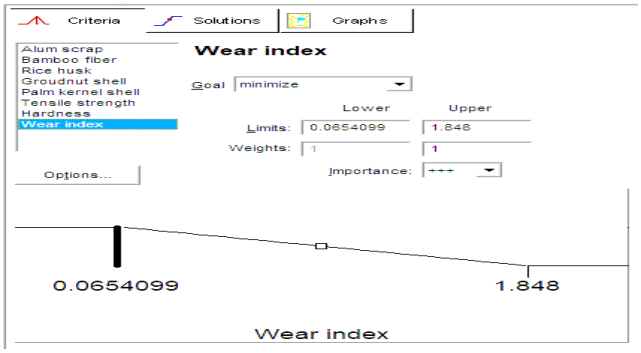

Figure 16: Optimization step for Wear Index

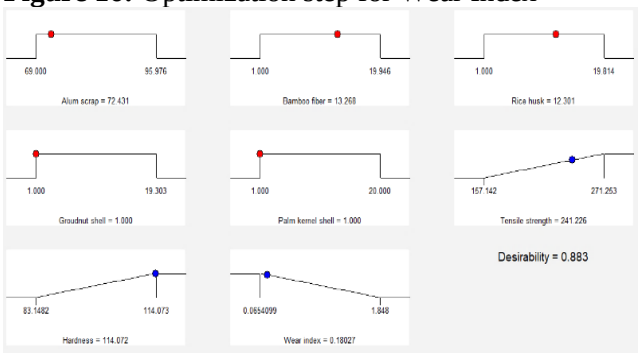

Figure 17: Solution to the optimization Problem

Table 19: The constraints for numerical optimization

Variables	Symbols	Goal	Lower limit	Upper limit	Lower weight	Upper weight	Importance
	Input variables/factors						
Aluminum scrap	A	is in range	69	96.0	1	1	3
Bamboo fiber	B	is in range	1	19.9	1	1	3
Rice husk	C	is in range	1	19.8	1	1	3
Groundnut shell	D	is in range	1	19.3	1	1	3
Palm kernel shell	E	is in range	1	20	1	1	3
	Output variables/responses						
Tensile strength	Y_1	Maximize	157.14	271.25	1	1	3
Hardness	Y_2	Maximize	83.15	114.07	1	1	3
Wear index (mg/rpm)	Y_5	Minimize	0.07	1.85	1	1	3

4.0 CONCLUSION

The D-Optimal Mixture Design Expert was successfully used for the optimization of the composite produced. It was found out that a blend of 72.43% weight of aluminium, 13.27% weight of Bamboo fibre, 12.30% weight of Rice Husk, 1.00% weight of Groundnut Shell and 1.00% weight of Palm kernel shell can be used to produce an Engineering composite material with a tensile strength of 241.23 MPa, hardness of 114.07 HV and wear index(rate) of 0.18 x 10^{-3} mg/rpm with a desirability of 88.30% and the model developed predicts the accuracy of tensile strength, hardness and wear index as 90.16%, 90.94% and 96.48% respectively. The Aluminum scrap provided a lightweight but strong matrix, while bamboo fiber and rice husk significantly enhanced tensile strength and hardness due to their high cellulose and silica

https://doi.org/10.4314/njt.2025.5184
http://creativecommons.org/licenses/by-nc-nd/4.0/

content [24]. The groundnut shell and palm kernel shell contributed to wear resistance and improved load-bearing capacity ([25], [26]). The optimized composition developed in this study offers a balance between mechanical strength, hardness, and wear resistance, rendering it suitable for applications requiring high durability, such as automotive and aerospace.

REFERENCES

[1] Fardin. K., Nayem. H., Juhi, J. M., SM Maksudur. R., Md. Jayed I., Mostakim B. and Mohammad, A. C. "Advances of composite materials in automobile applications – A review". *Journal of Engineering R Research, ELSEVIER*, 13(1), Pp. 1001–1023, 2025

[2] Oghoghorie O., Ebhojiaye R. S. and Amiolemhen P. E. "Assessment of The Wear Resistance and the Density Reduction of Aluminium When Reinforced with Coconut Shell Charcoal and Cow Bone Ash" World *Journal of Engineering Research and Technology (WJERT)*. 8(4), 27-40, 2022

[3] Ebhojiaye, R.S. and Eboigbe, C.I. Design and Analysis of 80cc, 4-Stroke Spark Ignition Engine Connecting Rod. *NIPES - Journal of Science and Technology Research*, *4*(2), 278-288, 2022

[4] Sarmah, P. and Gupta, K."Recent Advancements in Fabrication of Metal Matrix Composites: A Systematic Review"17(18), 4635,2024 https://doi.org/10.3390/ma17184635,

[5] Arulprasanna, A. and Omkumar, M "A review on composites: Selection and its applications" *Elsevier*, 2023 https://doi.org/10.1016/j.matpr.2024.06.014

[6] Montgomery, D. C. "Design and analysis of experiments". *John wiley & sons*. 2017

[7] Qi, B., Chen, X., Shen, F., Su, Y. and Wan, Y. "Optimization of Enzymatic Hydrolysis of Wheat Straw Pretreated by Alkaline Peroxide Using Response Surface Methodology". *Industrial & engineering chemistry research*, 48(15), 7346-7353, 2009

[8] Kyriazos, T. and Poga, M. "Dealing With Multicollinearity in Factor Analysis: The Problem, Detections, And Solutions". *Open Journal of Statistics*, 13(3), 404 - 424, 2023

[9] MacKinnon, J. G., Nielsen, M. O. and Webb, M. D. "Leverage, Influence and the Jackknife in Clustered Regression Models: Reliable Inference Using Summclust". *The Stata Journal*, 23(4), 942-982, 2023

[10] Myers, R. H., Montgomery, D. C., and Anderson-Cook, C. M. "Response Surface Methodology: Process and Product Optimization Using Designed Experiments (4thed.)". *Wiley*, 2016

[11] Box, G. E., Hunter, J. S., and Hunter, W. G. "Statistics for Experimenters". In Wiley series in probability and statistics. *Hoboken, NJ*: Wiley, 2022

[12] Eboigbe, C.I. and Ikponwosa-Eweka, O. "Optimization of Residual Stress in Mil Steel Gas Tungsten Arc welded joint using Response Surface Methodology". *Journal of Engineering for Development*, 13(2), 31 - 42, 2021

[13] Prasad, D. S., and Krishna, A. R. Tribological Properties of A356. 2/RHA Composites. Journal of Materials Science & Technology, 28(4), 367-372, 2012

[14] Aigbodion, V. S., and Hassan, S. B. "Experimental Correlations Between Wear Rate and Wear Parameter of Al–Cu–Mg/Bagasse Ash Particulate Composite". *Materials & Design*, 31(4), 2177-2180, 2010

[15] Alaneme, K. K., Bodunrin, M. O., and Awe, A. A. "Microstructure, Mechanical and Fracture Properties Of Groundnut Shell Ash And Silicon Carbide Dispersion Strengthened Aluminium Matrix Composites". *Journal of King Saud University-Eng. Sc.*, 30(1), 96-103, 2018

[16] Venkatesh, L., Arjunan, T. V., and Ravikumar, K. "Microstructural Characteristics and Mechanical Behaviour of Aluminium Hybrid Composites Reinforced with Groundnut Shell Ash and B4C". *Journal of the Brazilian Society of Mechanical Sciences and Engineering*, 41(7), 295, 2019. https://doi.org/10.1007/s40430-019-1800-1,

[17] Edoziuno, F. O., Adediran, A. A., Odoni, B. U., Utu, O. G., and Olayanju, A. "Physico-Chemical and Morphological Evaluation of Palm Kernel Shell Particulate Reinforced Aluminium Matrix Composites". *Materials Today: Proceedings*, 38, 652-657, 2021.

[18] Ikele, U. S., Alaneme, K. K., and Oyetunji, A. "Mechanical Behaviour of Stir Cast Aluminum Matrix Composites Reinforced with Silicon Carbide and Palm Kernel Shell Ash". *Manufacturing Review*, 9(12), 2022

[19] Hemmati, F., Farizeh, T., and Mohammadi-Roshandeh, J. "Lignocellulosic Fiber-Reinforced PLA Green Composites: Effects of Chemical Fiber Treatment". *Biocomposite*

Materials: Design and Mechanical Properties Characterization, 97-204, 2021.

[20] Nandiyanto, A. B. D., Hofifah, S. N., Girsang, G. C. S., Putri, S. R., Budiman, B. A., Triawan, F., and Al-Obaidi, A. S. M. "The Effects of Rice Husk Particles Size as a Reinforcement Component on Resin-Based Brake Pad Performance: From Literature Review on the Use of Agricultural Waste as a Reinforcement Material, Chemical P Polymerization Reaction of Epoxy Resin, To Experiments" *Automotive Experiences*, 4(2), 68-82, 2021

[21] Karam, D. S., Nagabovanalli, P., Rajoo, K. S., Ishak, C. F., Abdu, A., Rosli, Z., ... & Zulperi, D. "An Overview on The Preparation of Rice Husk Biochar, Factors Affecting Its Properties, and Its Agriculture Application". *Journal of the Saudi Society of Agricultural Sciences*, 21(3), 149-159, 2022

[22] Gehlen, G. D. S., Neis, P. D., Barros, L. Y. D., Poletto, J. C., Ferreira, N. F., and Amico, S. C. "Tribological Performance of Eco-Friendly Friction Materials With Rice Husk". *Wear*, 500, 204374, 2022

[23] Dinaharan, I., Gladston, J. A. K., Selvam, J. D. R., and Jen, T. C. "Influence Of Particle Content and Temperature on Dry Sliding Wear Behavior of Rice Husk Ash Reinforced AA6061 Slurry Cast Aluminum Matrix Composites". *Tribology International*, 183, 108406, 2023

[24] Dixit, P., and Suhane, A. "Aluminum Metal Matrix Composites Reinforced with Rice Husk Ash: A Review". *Materials Today: Proceedings*, 62, 4194-4201, 2022

[25] Sankaran, S., Palani, G., Yang, Y. L., And Trilaksana, H. "Enhancing Natural Fiber-Based Polymeric Composites with Biochar Filler Particles Derived from Groundnut Shell Biomass Waste". *Biomass Conversion and Biorefinery*,15(9):14399-14410,2024 Doi:10.1007/s13399-024-06201-0

[26] Sasirekha, S., Giridharan, K., and Chakravarthi, G. "Mechanical, Thermal Conductivity, And Water Absorption Properties of Biosilica and Palm Kernel Fiber Reinforced Vinyl Ester Composite Rebar for Building Materials". *Biomass Conversion and Biorefinery*, 14(16), 19973-19983, 2024